engineering proceedings

MDPI

Proceeding Paper

Numerical Study of a PVDF-Based Strain Sensor for Damage Detection of an Asphalt Concrete Pavement Subject to Dynamic Loads †

Jiayue Shen [1,*], Korkut Bekiroglu [1], Ali Tekeoglu [2], Ilker Boz [3], Weiru Chen [4] and Minghao Geng [5]

[1] Department of Engineering Technology, SUNY Polytechnic Institute, Utica, NY, USA; bekirok@sunypoly.edu
[2] Applied Physics Laboratory, Johns Hopkins University, Columbia, MD, USA; ali.tekeoglu@jhuapl.edu
[3] Virginia Transportation Research Council, Charlottesville, VA, USA; ilker.boz@vdot.virginia.gov
[4] Department of Computer and Information Science, Arkansas Tech University, Russellville, AR, USA; wchen7@atu.edu
[5] Department of Computer Science, SUNY Polytechnic Institute, Utica, NY, USA; gengm@sunypoly.edu
* Correspondence: shenj@sunypoly.edu; Tel.: +1-315-351-3531
† Presented at the 9th International Electronic Conference on Sensors and Applications, 1–15 November 2022; Available online: https://ecsa-9.sciforum.net/.

Abstract: This paper studies the performance of Polyvinylidene fluoride (PVDF)–based strain sensor subject to dynamic loads with different load-moving velocities and the strain sensor's performance for bottom-up crack detection of an asphalt pavement subject to dynamic loads. The core of the strain sensor is a metalized PVDF sensing film packaged with three protection layers. The encapsulated strain sensor adopts an H-shape to optimize the overall performance. Two numerical models are built in this paper and validated that the voltage output of the PVDF-based strain sensor can well capture the peak lateral strain with the propagation of the bottom-up cracks or the variation of a load moving velocity. And the sensor has better performance when it is in its lateral alignment position.

Keywords: strain sensor; PVDF; asphalt pavement; structural health monitoring; damage detection

Citation: Shen, J.; Bekiroglu, K.; Tekeoglu, A.; Boz, I.; Chen, W.; Geng, M. Numerical Study of a PVDF-Based Strain Sensor for Damage Detection of an Asphalt Concrete Pavement Subject to Dynamic Loads. *Eng. Proc.* **2022**, *4*, x. https://doi.org/10.3390/xxxxx

Academic Editor: Francisco Falcone

Published: 1 November 2022

Publisher's Note: MDPI stays neutral with regard to jurisdictional claims in published maps and institutional affiliations.

1. Introduction

As one of the essential components of the road infrastructure, the health condition of the asphalt concrete pavement affects the safety and quality of transportation. Due to main causes, such as vibration induced by the traffic, work zone, or natural events, reflective crack from an underlying layer, asphalt binding aging, etc. [1], the asphalt concrete pavement fails on the top-down cracks and bottom-up cracks. And sometimes, surface failure may be caused by bottom-up cracks, which are usually challenging to be identified and localized. So it is critical to offer continuously structural health monitoring of the asphalt concrete pavement using a non-destructive and cost-effective approach that can better detect defects of the bottom-up cracks and boost timely maintenance.

Nowadays, three prominent technologies are utilized by researchers to detect bottom-up cracks: Ground Penetrating Radar (GPR) [2,3], ultrasonic technology [4,5], and in-pavement sensing technology [6,7]. GPR is a non-deconstructive technique that utilizes the difference in electromagnetic properties of the underground medium, reflections, and transmissions of electromagnetic waves generated at the interfaces of different electrical interfaces for measuring the targeting objects. Within a limited depth, GPR can offer three-dimensional scanning of the pavement. However, it is difficult for GPR to accurately estimate the cracks when the pavement is thick or has high humidity [8,9]. Ultrasonic technology calculates the time from the start ultrasonic stress-wave pulse to the arrival of echo

reflection for detecting cracks and joints in asphalt concrete pavement [10,11]. Ultrasonic technology allows to detect the pavement distresses at a mid-depth level. With the recurrence plot quantification analysis method, the reliability and sensitivity of the ultrasonic technology can be improved in the damage detection of non-homogeneous materials [12]. The ultrasonic technology is still constrained by environmental conditions, such as the moisture level in the pavement and weather changes, e.g., different material properties may be detected for the same material under different weather conditions due to its low transmission capability [13,14]. In-pavement sensing technology usually measures cracks and road conditions using sensor arrays. One of the most popular sensors for damage detection is a strain gauge, including optical fiber [14], conventional electrical resistance strain gauge [15], metal-foil gauges [16], and so on. Due to the harsh installation conditions of asphalt concrete pavement, high temperatures (up to 164 °C), and pressure (around 290 ksi) [17,18], Metal-foil gauges are rarely used for asphalt concrete pavement. The conventional electrical resistance strain gauge is commonly used in asphalt pavement, but its installation requires digging holes in the pavement and then to be sealed the strain gauge in the pavement using the cold patch, which material properties are different from the original asphalt concrete mixture and further affect the results for damage detection. Optical fiber can offer accurate measurement, but the cost is relatively high [15].

Piezoelectric plastic materials, e.g., PVDF, which can generate electrical charges when mechanically deformed, are commonly used for concrete structural health monitoring [19]. It offers the advantages of high sensitivity, good flexibility, good manufacturability, small distortion, low thermal conductivity, high chemical corrosion resistance, and heat resistance. The authors have proposed a cost-effective piezoelectric-based strain sensor for damage detection of asphalt pavement [20]. This paper further studies the performance of strain sensors subject to dynamic loads with different load-moving velocities and the strain sensor's performance for bottom-up crack detection of an asphalt pavement subject to dynamic loads. Section 2 briefly introduces the study's sensor configuration and the finite element model. Section 3 elaborates on the results and discussion. The last section is the conclusion.

2. Materials and Methods

2.1. Sensor Configuration

The sensor designed in this paper is shown in Figure 1, which is validated by the authors' previous study [20]. The outer layer uses epoxy resin as a coating layer, followed by polyurethane foam as a thermal insulation layer(thickness is 11 mm), and then an epoxy layer on the inside(thickness is 10 mm). The inner layer is PVDF (key sensing unit), and the size is 80 mm × 18 mm × 1 mm. The shape of the sensor is H-shape because H-shape can make the whole sensor better sense the change of road surface and can transfer the deformation to the key sensing unit very effectively. The ratio of middle beam length to side-wing length is 3.2, which is the best ratio to detect pavement deformation. In order to overcome the high temperature of the sensor during the installation process, polyurethane foam is chosen as the insulation layer to be added to the outer layer. Araldite GY-6010 epoxy resin is selected as the material of epoxy resin because it has high tensile strength and flexural strength, as well as good heat insulation performance.

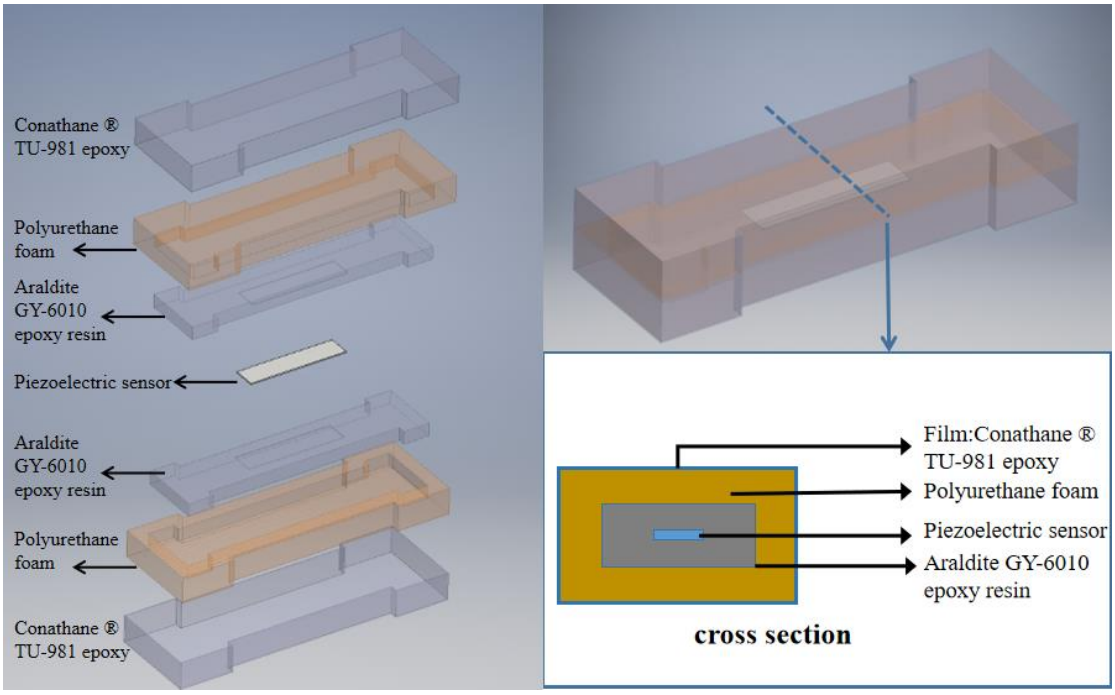

Figure 1. Configuration of the strain sensor.

2.2. Finite Element Model

The paper established and simulated two sets of FEM in COMSOL Multiphysics, as shown in Figure 2a. In the first FEM study, with no bottom-up crack existing in the asphalt concrete pavement, the sensor output signal and measured strain at the bottom of the pavement in response to the load moving velocity are investigated. The moving speed of the same dynamic load varies from 25 km/h to 75 km/h with an increment of 10 km/h. In the second FEM study, a bottom-up crack initiates at the center of the bottom surface of the pavement along the *x*-axis. The crack depths vary from 0 cm (0 inches) to 7.62 cm (3 inches) with 1.27 cm (0.5 inches) increments. In the FEM, the same dynamic load with a fixed load moving velocity is applied on the top surface of the pavement, as shown in Figure 2a. In addition, the sensor is placed in two directions (horizontal and vertical) for both FEM studies, as shown in Figure 2b, for studying the impact of the sensor alignment in response to the bottom-up crack detection.

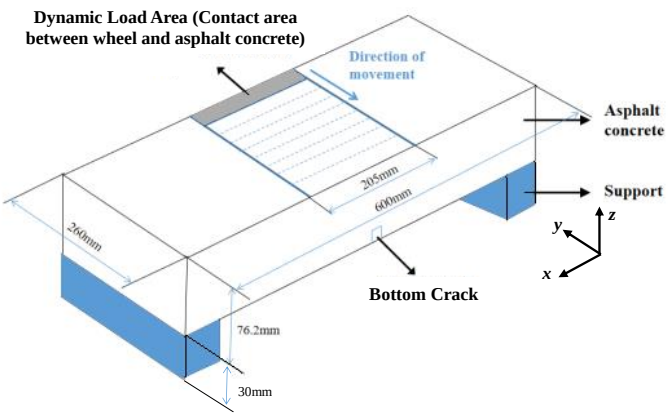

(**a**)

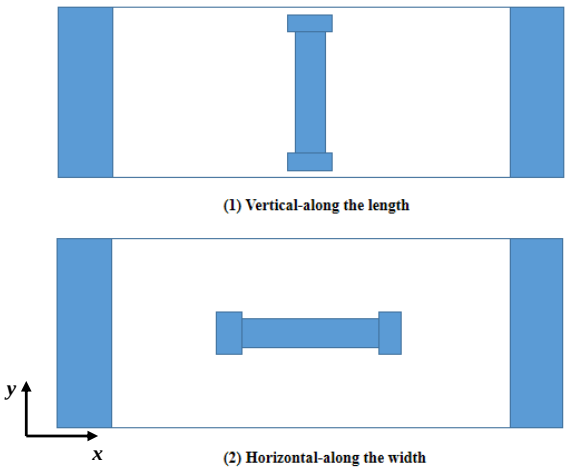

(**b**)

Figure 2. (**a**) Schematic of the numerical model of a dynamic load passing through the road surface. (**b**) Bottom view of the numerical model for showing sensor alignment.

In both FEM studies, the asphalt concrete pavement is with a size of 600 mm × 260 mm × 76.2 mm. Two supports are placed at two ends of the pavement bottom. A customized strain sensor is attached underneath the center of the bottom surface of the asphalt concrete pavement, as shown in Figure 2a. This paper subdivides the grid for the strain sensor to better investigate the sensor's responses to sensing the bottom-up cracks. During the dynamic simulation, a dynamic load is applied to the middle region of the upper surface of the asphalt concrete pavement. And the contact area of the dynamic load on the pavement surface is 215 mm* 30 mm to mimic the contact area of a car tire on the pavement in an actual application. In addition, the dynamic load chooses 90.72 tons (200 kips) to mimic the weight of a moving overweighed truck [21]. In the FEM, asphalt concrete is simulated as a viscoelastic material. As such, the asphalt concrete's shear modulus and relaxation time are set as 10 MPa and 0.3 s in the FEM, respectively. The properties of each material are shown in Table 1.

Table 1. Key material properties used in FEM.

Material	Density (kg/m^3)	Young's Modulus (GPa)	Poisson's Ratio
Asphalt concrete	2402.77	12	0.3
Polyurethane foam	50	0.151	0.37
Araldite GY-6010 epoxy resin	2700	2.067	0.37
Piezoelectric sensor	1780	2	0.39

3. Results and Discussion

Figure 3a,b show the measured strain sensor output and the measured lateral strain (along the *x*-axis) in response to different load-moving velocities when there is no crack existing in the pavement. The strain sensor is aligned vertically (along the *y*-axis) in Figure 3a and laterally (along the *x*-axis) in Figure 3b. Figure 3a,b indicate that the measured sensor output has the same trend as the lateral strain, which means the strain sensor, no matter if it is aligned vertically or laterally, can accurately capture the lateral strain of the pavement. However, Figure 3a,b also show that the strain sensor is more sensitive to lateral strain when the strain sensor is aligned laterally.

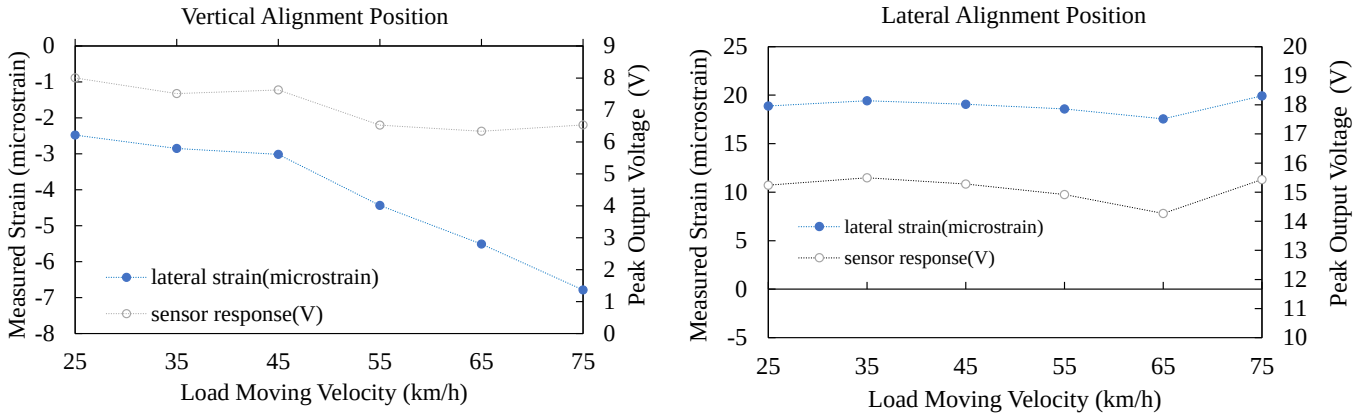

(**a**) (**b**)

Figure 3. Measured lateral strain (along the *x*-axis) and peak piezoelectric-based sensor output in response to the dynamic load moving velocity when there is no bottom-up crack existing in the

asphalt concrete pavement (crack depth = 0 cm): (**a**) sensor is vertical aligned (along the *y*-axis); (**b**) senor is lateral aligned (along the *x*-axis).

In Figure 3a, the sensor is aligned vertically. The sensor output decreases when the load moving velocity increases from 25 km/h to 35 km/h and from 45 km/h to 65 km/h, and increases slightly when the load moving velocity increases from 35 km/h to 45 km/h and from 65 km/h to 75 km/h. Please notice that the measured lateral strain is negative. So the trend of the absolute value of the lateral strain is precisely opposite to the sensor output except when the load moving velocity is from 65 km/h to 75 km/h. The reason should be that the pavement structure in FEM reaches its resonance frequency when the load moving velocity is from 65 km/h to 75 km/h.

In Figure 3b, the sensor is aligned laterally. The sensor output increases slightly when the load moving velocity increases from 25 km/h to 35 km/h and from 65 km/h to 75 km/h, and decreases continuously when the load moving velocity increases from 35 km/h to 65 km/h. The lateral strain measured above the sensor also shows the same trend. Similarly, the reason should be that the pavement structure in FEM reaches its resonance frequency when the load moving velocity is from 65 km/h to 75 km/h.

Figure 4a,b show measured lateral strain (along the *x*-axis) and peak piezoelectric-based sensor output in response to the depth of the bottom-up crack when the dynamic load moving velocity equals 25 km/h. The strain sensor is aligned vertically (along the *y*-axis) in Figure 4a and laterally (along the *x*-axis) in Figure 4b. Before the crack depth reaches the whole pavement thickness, the trend of the sensor output is totally aligned with the trend of the lateral strain, no matter whether the sensor is aligned vertically or laterally, as shown in Figure 4a,b. When the pavement completely breaks (the crack depth=the pavement thickness), the decreasing trend of lateral strain is captured by the sensor output in Figure 4b but not well represented by the sensor output in Figure 4a. In other words, the strain sensor output can better capture the strain change with lateral alignment position. Also, sensor output and lateral strain are much larger when the sensor output is in a lateral alignment position.

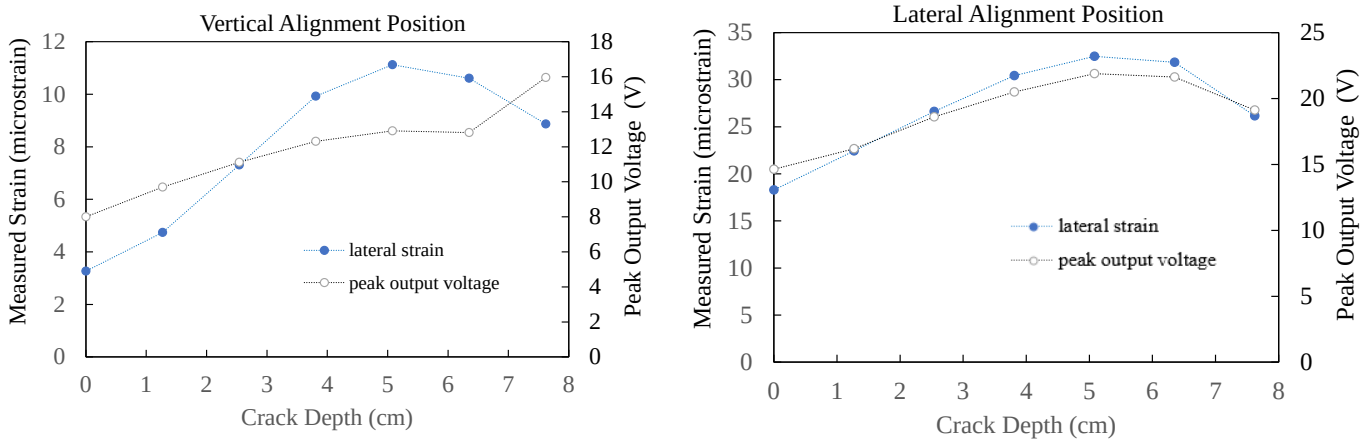

(**a**) (**b**)

Figure 4. Measured lateral strain (along the *x*-axis) and peak piezoelectric-based sensor output in response to the depth of the bottom-up crack when the dynamic load moving velocity equals 25 km/h: (**a**) sensor is vertical aligned (along the *y*-axis); (**b**) senor is lateral aligned (along the *x*-axis).

In Figure 4a, when the crack depths initiate and propagate from 0 cm (0 in) to 5.08 cm (2 in), both sensor output and lateral strain gradually go up. When the crack depth propagates from 5.08 cm (2 in) to 6.35 cm (2.5 in), the sensor output and lateral strain show a decreasing trend. Then the lateral strain continuously decreases but the sensor output increases when the crack depth grows from 6.35 cm (2.5 in) to 7.62 (3 in).

In Figure 4b, the sensor output and measured lateral strain increase almost linearly with the increase of the crack depth from 0 cm (0 in) to 3.81 cm (1.5 in). Then the increasing trend slows down when the crack depth increase from 3.81 cm (1.5 in) to 5.08 cm (2 in). The measured lateral strain and sensor output reduce with an increasing trend of the crack depth from 5.08 cm (2 in) to 7.62 cm (3 in). In Figure 4a,b, the measured lateral strain has a similar trend no matter whether the strain sensor is aligned vertically or laterally. But the measured lateral strain is much more prominent when the strain sensor is aligned laterally.

4. Conclusions

This paper studies the proposed strain sensor subject to dynamic loads with different load-moving velocities and the strain sensor's performance for bottom-up cracks detection of an asphalt pavement subject to dynamic loads. The results validate that the proposed strain sensor can differential the load moving velocity by the measured lateral strain. And the strain sensor also can detect the initiation and propagation of a bottom-up crack and capture the peak of the lateral strain before the pavement is entirely broken. Both numerical studies indicate that the sensor has better outputs when aligned laterally.

Author Contributions: Conceptualization, J.S., K.B., A.T. and I.B.; methodology, J.S.; software, M.G.; validation, J.S. and W.C.; formal analysis, J.S., M.G. and W.C.; investigation, J.S., K.B. and A.T.; resources, I.B.; data curation, J.S.; writing—original draft preparation, J.S.; writing—review and editing, K.B., A.T. and I.B.; visualization, J.S.; supervision, J.S.; project administration, J.S.; funding acquisition, J.S., K.B., A.T. and I.B. All authors have read and agreed to the published version of the manuscript.

Funding: This research was funded by the 2020 Virginia Transportation Research Council Award #116019.

Institutional Review Board Statement:

Informed Consent Statement:

Data Availability Statement: Not applicable.

Acknowledgments: Not applicable.

Conflicts of Interest: The authors declare no conflict of interest.

References

1. Adlinge, S.S.; Gupta, A. Pavement deterioration and its causes. *Int. J. Innov. Res. Dev.* **2013**, *2*, 437–450.
2. Salvi, R.; Ramdasi, A.; Kolekar, Y.A.; Bhandarkar, L.V. Use of ground-penetrating radar (GPR) as an effective tool in assessing pavements—A review. *Geotech. Transp. Infrastruct.* **2019**, 85–95. https://doi.org/10.1007/978-981-13-6713-7_7.
3. Georgiou, P.; Loizos, A. Parametric optimization of ground penetrating radar approach for assessing asphalt pavement surface layers compaction. *J. Appl. Geophys.* **2020**, *182*, 104187. https://doi.org/10.1016/j.jappgeo.2020.104187.
4. Behera, H.K.; Pradhan, S.; Das, S.S. Low cost ultrasonic roughometer for pavement roughness measurement. *Innov. Infrastruct. Solut.* **2021**, *6*, 1–13. https://doi.org/10.1007/s41062-021-00521-0.
5. du Tertre, A.; Serhan Kırlangıç, A.; Cascante, G.; Tighe, S.L. A non-destructive approach for the predictive master curve of ASPHALT pavements using ultrasonic and deflection methods. *Int. J. Pavement Eng.* **2022**, *23*, 1540–1551. https://doi.org/10.1080/10298436.2020.1810687.
6. Ma, X.; Dong, Z.; Dong, Y. Toward asphalt pavement health monitoring with built-in sensors: A novel application to real-time modulus evaluation. *IEEE Trans. Intell. Transp. Syst.* **2021**. https://doi.org/10.1109/tits.2021.3102252.
7. Liu, Z.; Gu, X.; Wu, C.; Ren, H.; Zhou, Z.; Tang, S. Studies on the validity of strain sensors for pavement monitoring: A case study for a fiber Bragg grating sensor and resistive sensor. *Constr. Build. Mater.* **2022**, *321*, 126085. https://doi.org/10.1016/j.conbuildmat.2021.126085.
8. Benedetto, A. A three dimensional approach for tracking cracks in bridges using GPR. *J. Appl. Geophys.* **2013**, *97*, 37–44. https://doi.org/10.1016/j.jappgeo.2012.12.010.
9. Luburić, I.; Perić, Z.; Šesnić, S. Electromagnetic modeling of the GPR response to the pipe system set in the concrete slab. In Proceedings of the 2017 25th International Conference on Software, Telecommunications and Computer Networks (SoftCOM), 2017; pp. 1–5. https://doi.org/10.23919/softcom.2017.8115531.

10. du Tertre, A.; Kırlangıç, A.S.; Cascante, G.; Tighe, S.L. Ultrasonic inspection of asphalt pavements to assess longitudinal joints. *Road Mater. Pavement Des.* **2022**, *23*, 129–148. https://doi.org/10.1080/14680629.2020.1820895.
11. Pan, W.-H.; Sun, X.-D.; Wu, L.-M.; Yang, K.-K.; Tang, N. Damage detection of asphalt concrete using piezo-ultrasonic wave technology. *Materials* **2019**, *12*, 443. https://doi.org/10.3390/ma12030443.
12. Carrión, A.; Genovés, V.; Gosálbez, J.; Miralles, R.; Payá, J. Ultrasonic signal modality: A novel approach for concrete damage evaluation. *Cem. Concr. Res.* **2017**, *101*, 25–32. https://doi.org/10.1016/j.cemconres.2017.08.011.
13. Al-Qadi, I.L.; Sebaaly, P.E.; Wambold, J.C. *New and Old Technology Available for Pavement Management System to Determine Pavement Condition*; ASTM International: West Conshohocken, PA, USA, 1991. https://doi.org/10.1520/stp17818s.
14. Salles, L.; Balbo, J.T.; Khazanovich, L. Non-destructive ultrasonic tomography for concrete pavement evaluation: Signal processing and image analysis of crucial parameters. *Rev. IBRACON De Estrut. E Mater.* **2017**, *10*, 1182–1191. https://doi.org/10.1590/s1983-41952017000600004.
15. Lydon, M.; Taylor, S.E.; Robinson, D.; Callender, P.; Doherty, C.; Grattan, S.K.; O'Brien, E.J. Development of a bridge weigh-in-motion sensor: Performance comparison using fiber optic and electric resistance strain sensor systems. *IEEE Sens. J.* **2014**, *14*, 4284–4296. https://doi.org/10.1109/jsen.2014.2332874.
16. Zhao, H.; Wu, C.; Wang, X.; Zheng, Y. Pavement condition monitoring system at shanghai pudong international airport. In *Pavement Materials, Structures, and Performance*; 2014; pp. 283–295. https://doi.org/10.1061/9780784413418.029.
17. Lajnef, N.; Chatti, K.; Chakrabartty, S.; Rhimi, M.; Sarkar, P. *Smart Pavement Monitoring System*; United States. Federal Highway Administration: 2013.
18. Kim, Y.R.; Seo, Y.; King, M.; Momen, M. Dynamic modulus testing of asphalt concrete in indirect tension mode. *Transp. Res. Rec.* **2004**, *1891*, 163–173. https://doi.org/10.3141/1891-19.
19. Du, G.; Li, Z.; Song, G. A PVDF-based sensor for internal stress monitoring of a concrete-filled steel tubular (CFST) column subject to impact loads. *Sensors* **2018**, *18*, 1682. https://doi.org/10.3390/s18061682.
20. Shen, J.; Geng, M.; Schultz, A.; Chen, W.; Qiu, H.; Wang, X. Numerical Study of a Multi-Layered Strain Sensor for Structural Health Monitoring of Asphalt Pavement. *Multidiscip. Digit. Publ. Inst. Proc.* **2019**, *42*, 41. https://doi.org/10.3390/ecsa-6-06527.
21. Nowak, A.S.; Laman, J.A.; Nassif, H. *Effect of Truck Loading on Bridges*; United States. Michigan Department of Transportation: 1994.